Plant Soil
https://doi.org/10.1007/s11104-026-08906-9

RESEARCH ARTICLE

Metal hyperaccumulation and distribution in *Anthyllis vulneraria* from Cave del Predil: zinc or thallium?

Ksenija Jakovljević · Cristina Gonnelli · Gaia Regini · Marco Dainelli · Dennis Brückner · Pablo Carril · Nadia Bazihizina · Ilaria Colzi · Laura Pilotto · Luca Marchiol · Mirko Salinitro · Antony van der Ent

Received: 10 June 2026 / Accepted: 15 July 2026
© The Author(s), under exclusive licence to Springer Nature Switzerland AG 2026

Abstract

Background and aims *Anthyllis vulneraria*, a common and widespread legume in Europe, spontaneously colonizes metalliferous habitats highly enriched in thallium and zinc, with hyperaccumulation of these elements reported in its subspecies from some populations.

Methods Metallicolous and non-metallicolous accessions of *Anthyllis vulneraria* subsp. *polyphylla* from northeast Italy were cultivated hydroponically and exposed to different concentrations of zinc and thallium to assess thallium and zinc accumulation in the plants and to analyze the effects on growth and photosynthetic efficiency. Synchrotron X-ray fluorescence microscopy was used to elucidate elemental distribution at the cellular level in plant organs in field-collected plants.

Results Synchrotron X-ray fluorescence microscopy revealed distinct localization of zinc and thallium in the epidermis of the root and petiole, as well as in the vasculature of the leaves. In the zinc treatment in hydroponics, root concentrations were significantly higher than in the shoots for both accessions, reaching the highest value when dosed with 2000 µM zinc, with 4000 µg g^{-1} in the shoot and 11,000 µg g^{-1} in the roots of *Anthyllis vulneraria* subsp. *polyphylla*. In contrast, in both thallium treatments, the shoot:root ratio was greater than one. Photosynthetic activity and plant growth were reduced in the non-metallicolous population, whereas in the metallicolous population it remained largely stable across the treatments.

Conclusion The spatial distribution of zinc and thallium in field-collected plants has features typical of metal hyperaccumulators, such as preferential accumulation in the epidermal cells. Under controlled

Responsible Editor: Michel-Pierre Faucon.

Ksenija Jakovljević and Cristina Gonnelli joint first authors.

Supplementary Information The online version contains supplementary material available at https://doi.org/10.1007/s11104-026-08906-9.

K. Jakovljević
Department of Ecology, Institute for Biological Research Siniša Stanković – National Institute of the Republic of Serbia, University of Belgrade, Belgrade, Serbia

C. Gonnelli · G. Regini · M. Dainelli · P. Carril · N. Bazihizina · I. Colzi
Department of Biology, Università degli Studi di Firenze, Florence, Italy

D. Brückner
Deutsches Elektronen-Synchrotron, Hamburg, Germany

L. Pilotto · L. Marchiol
Department of Agrifood, Environmental and Animal Sciences, University of Udine, Udine, Italy

M. Salinitro · A. van der Ent (✉)
Laboratory of Genetics, Wageningen University and Research, Wageningen, The Netherlands
e-mail: antony.vanderent@wur.nl

Published online: 04 August 2026

conditions genuine hyperaccumulation was shown only for thallium, while exclusion mechanisms combined with high internal tolerance were found for zinc.

Keywords Accumulation · Exclusion · Legume · Localization · Tolerance

Introduction

Thallium (Tl) toxicity is famous on account of its historical use as a biocidal agent in pest control and in criminal poisoning cases (Kazantzis 2000; Li et al. 2026). The occurrence and behaviour of Tl as an environmental pollutant remains understudied compared to other inorganic contaminants, such as arsenic (As), mercury (Hg), lead (Pb) or cadmium (Cd) (Zhong et al. 2022). Thallium is attracting increased attention due to recognition of its potential harmful effects in the environment, and its use in advanced technology-critical materials with applications in infrared lenses/glasses, superconductors and radiation detection (Liu et al. 2019; US Geological Survey 2026). Anthropogenic sources account of Tl for the largest proportion of the annual total Tl release in the environment, estimated at 2000–5000 t (Ostrander et al. 2024; Peter and Viraraghavan 2005), and include mining and smelting of sulphide ores, coal combustion, waste incineration, cement production, *etc*. (Liu et al. 2024). Natural sources of Tl are rare, with the Lanmuchang deposit in China and the Allchar deposit in North Macedonia being the richest known occurences, with up to 124 μg g^{-1} in soils from the mining area of Lanmuchang (Xiao et al. 2012) and up to 20 mg g^{-1} in Allchar soil (Bačeva et al. 2014). Other sites with localized Tl enriched mineralization occur in Northern Italy, France, southern Poland, Switzerland and the USA (Migaszewski and Gałuszka 2021). Most Tl occurs in sulfide ores, such as galena, sphalerite, and pyrite, and consequently enrichment has been reported in association with Zn-Pb–Cd sulfide ore deposits (Karbowska 2016; Xiao et al. 2012). In nature, Tl occurs in two valences (Tl^+ and Tl^{3+}), with the instable Tl^{3+} being far more toxic (Ralph and Twiss 2002). The more stable Tl^+ is, however, more bioavailable and, due to its chemical similarity to potassium, is more readily taken up by plants (Karbowska 2016; Pošćić et al. 2013).

Thallium hyperaccumulators, species with foliar concentrations exceeding the threshold for hyperaccumulation of 100 μg g^{-1}, have been found at two Zn-Pb mine sites in Northern Italy and France respectively (Escarré et al. 2011; Fellet et al. 2012; Pošćić et al. 2015; Regini et al. 2026), and at the Tl-Sb-As deposit of Allchar in North Macedonia (Jakovljević et al. 2025a). In the leaves of *Silene latifolia* from Allchar, the highest known concentration of Tl in a plant has been reported, reaching up to 80,000 μg g^{-1} (Jakovljević et al. 2025a). Foliar concentrations in *Biscutella laevigata* from Cave del Predil (Zn-Pb mine in Northern Italy) can exceed 32,000 μg g^{-1} (Fellet et al. 2012), whereas the leaves of *Iberis intermedia* from Les Malines in Southern France had nearly 3000 μg g^{-1} (Leblanc et al. 1999). Despite the anomalous concentrations of Zn, Pb, Cd and Tl in the soil (total Tl up to 9000 μg g^{-1}, 66,000 μg g^{-1} Zn and 60,000 μg g^{-1} Pb in the Cave del Predil and 245 μg g^{-1} Tl, 160,000 μg g^{-1} Zn and 9700 μg g^{-1} Pb in the Les Malines area; Escarré et al. 2011; Fellet et al. 2012), Les Malines and Cave del Predil harbour diverse vascular floras. Apart from *B. laevigata*, *I. intermedia* and *S. latifolia*, this includes hyperaccumulators, such as *Minuartia verna*, *Anthyllis vulneraria*, as well as *Noccaea cepaeifolia*, *Alyssum wulfenianum* (Cave del Predil) and *Noccaea caerulescens* (Les Malines) (Escarré et al. 2011; Fellet et al. 2012; Reeves and Brooks 1983).

Hyperaccumulation of more than one element simultaneously is rare, and mainly known from species in the genus *Noccaea* in which many species can co-accumulate Zn, nickel (Ni) and/or Cd and in *Arabidopsis halleri* which can co-accumulate Zn and Cd (Reeves et al. 2001; Stein et al. 2017), with both positive and negative correlations in co-accumulation (Dilshara et al. 2024; Kozhevnikova et al. 2020; Richau and Schat 2009; Tang et al. 2019). In areas rich in Tl and Zn, Zn concentrations considerably exceeded the threshold for hyperaccumulation in *A. vulneraria* and *N. caerulescens* from Les Malines (Escarré et al. 2011) and in *M. verna* and *N. cepaeifolia* (*N. rotundifolia* complex) from Cave del Predil (Fellet et al. 2012), with more than 10,000 Zn g^{-1} d.w. in the leaves and a shoot:root ratio higher than one in the latter. The hyperaccumulation threshold in plants in the Les Malines area was also exceeded in *Alyssum serpyllifolium* with 3500 μg Zn g^{-1} d.w. and in

B. laevigata (Escarré et al. 2011) which also has high foliar Zn concentrations at Cave del Predil (Fellet et al. 2012; Reeves and Brooks 1983).

Anthyllis vulneraria is one of very few hyperaccumulating legumes, with high Zn and Tl reported in different *A. vulneraria* subspecies: on Zn-Pb enriched soils at Les Malines individual plants of *A. vulneraria* subsp. *carpatica* accumulated up to 10,000 µg g^{-1} Zn (Escarré et al. 2011), whereas in the leaves of *A. vulneraria* from the Allchar site 1220 µg g^{-1} Tl has been recorded (Jakovljević et al. 2025a). However, when *A. vulneraria* subsp. *polyphylla* from Cave del Predil in Italy was grown experimentally in its native soil with no amendments, both Tl and Zn shoot concentrations were above the hyperaccumulation thresholds (733 µg g^{-1} Tl and 3360 µg g^{-1} Zn; Fellet et al. 2014), but only Tl was preferentially accumulated in the aboveground tissues. Apart from *A. vulneraria*, within the family Fabaceae hyperaccumulation is principally known from numerous selenium (Se) hyperaccumulating taxa in the genus *Astragalus* on seleniferous soils in the United States (White 2016). Furthermore, in Australia, the legume *Crotalaria novae-hollandiae* from the Dugald River Zn-Pb–Cd gossan in central Queensland is a facultative polymetallic Zn-Cu-Cd hyperaccumulator accumulating up to 16,200 µg Zn g^{-1}, 545 µg Cu g^{-1} and 170 µg Cd g^{-1} (Farago et al. 1977; Tang et al. 2022a, b). Another species in this genus, *C. cobalticola* is a Cu-Co obligate hyperaccumulator found in the DR Congo (Brooks et al. 1977; Brooks 1979). Finally, Ni hyperaccumulation in another legume *Pearsonia metallifera* with up to µg Ni g^{-1}, has been recorded in Zimbabwe (Brooks and Yang 1984).

The hyperaccumulation capacity and high biomass production of *A. vulneraria* make it a promising candidate for phytoextraction; in particular, *A. vulneraria* plant material has been developed as an Eco-Zn catalyst (Grison et al. 2015). It exhibits more favorable characteristics compared with hyperaccumulators such as *N. caerulescens*, with greater selectivity for Cd and Pb, and, after inoculation with *Rhizobium metallidurans*, accumulation increases by more than 30% (Grison et al. 2015). Conversely, in symbiosis with *Mesorhizobium* strains, Zn accumulation in *A. vulneraria* subsp. *carpatica* significantly reduced (Soussou et al. 2013), indicating differential responses to the presence of rhizobia and providing new perspectives for unravelling the role of bacteria in modulating Zn uptake, translocation, and accumulation in host plants. In addition to revegetation and restoration of mine areas (Mahieu et al. 2013), spontaneous colonization of mine areas by Fabaceae species is particularly important because their increased nitrogen content and enhanced organic matter accumulation, arising from their symbiotic relationship with nitrogen-fixing bacteria, both improve soil fertility (Sujkowska-Rybkowska et al. 2020). In symbiosis with the highly metal-tolerant *Mesorhizobium metallidurans*, *Anthyllis vulneraria* subsp. *carpatica* achieved nitrogen fixation of 80% (Mahieu et al. 2011), while the nitrogen input from *A. vulneraria* during a four-year experiment was estimated at 400 kg ha^{-1}, facilitating the growth of neighboring species (Escarré et al. 2011).

Anthyllis vulneraria is a very widespread and common species throughout Europe, and metal-tolerance and metal accumulation in several populations raises questions about the evolution of metal tolerance in this species when colonizing metalliferous habitats. Specifically, of interest is to elucidate the underlying molecular and physiological mechanisms for co-accumulating not only Zn, but also Tl in some populations, notably Cave del Predil. Therefore, in this ecophysiological study we set out to determine the tolerance and accumulation capacity for Tl and Zn of the metallicolous population from Cave del Predil. This was done under controlled conditions in hydroponics to allow precise exposure without confounding factors arising from metal availability. To provide a reference, we compared the metallicolous population with a non-metallicolous *A. vulneraria* population from San Osvaldo in the same geographical area. We assessed plant growth and photosynthetic parameters and determined the distribution of Tl and Zn at the tissue and cellular levels in field-collected plants.

Materials and methods

Collection of plant material in the field

Plant material and seeds of *Anthyllis vulneraria* subsp. *polyphylla* (DC.) Nyman were collected from natural populations in July 2025 at Cave del Predil, a former Zn-Pb mine site (metallicolous), and at a control site at San Osvaldo (non-metallicolous), both located in North-East Italy. Information about the localities and populations is given in Table 1.

Table 1 Characterization of collection sites of *Anthyllis vulneraria* subsp. *polyphylla*, with Zn and Tl concentrations (μg g^{-1} d.w.) in soils and shoots of field collected plants (values are means of 5 replicates ± standard deviation)

Population	Coordinates (Lat, Long)	Substrate	[Zn] soil	[Zn] shoot	[Tl] soil	[Tl] shoot
San Osvaldo non-metallicolous	46° 03′ 44″ N 13° 22′ 73″ E	Calcareous soil	57 ± 13	48 ± 20	b.d.l	b.d.l
Cave del Predil metallicolous	46° 26′ 30″ N 13° 34′ 10″ E	Metalliferous soil	15,060 ± 690	4530 ± 2690	125 ± 12	1960 ± 690

b.d.l. below detection limit

Synchrotron μXRF experiments

The X-ray fluorescence microscopy and microtomography (XRF-μCT) analyses of field-collected *A. vulneraria* subsp. *polyphylla* were conducted at PETRA III (Deutsches Elektronen-Synchrotron, DESY), a 6 GeV synchrotron radiation source, specifically at the hard X-ray microprobe experiment at the undulator beamline P06 (Boesenberg et al. 2016). The P06 beamline is equipped with a cryogenically cooled Si (111) double-crystal monochromator. An ion chamber upstream of the sample monitors the incoming flux, while a 500 μm-thick Si PIPS diode with a 19 mm-diameter active area [PD300-500CB, Mirion Technologies (Canberra) GmbH, Germany] located downstream of the sample records the transmitted X-ray intensity to extract absorption data. A pair of Kirkpatrick-Baez mirrors was used to focus the 16 keV X-ray beam down to approximately 440 nm × 300 nm (horizontal × vertical) for the tomographic measurements or 460 nm × 400 nm (horizontal × vertical) for the 2D measurements, resulting in a flux of about 8.0×10^9 photons s^{-1} or 7.6×10^9 photons s^{-1} on the sample, respectively. Detection of XRF during the tomography measurements was performed using a four-element Vortex silicon drift detector (Hitachi High-Tech, USA) and a 16-element Ardesia silicon drift detector (Politecnico di Milano), placed at 90° and 270°, respectively, with the forward direction of the X-ray beam defined as 0°. During the 2D measurements, the XRF signal was detected using a 16-element Ascanio silicon drift detector (Politecnico di Milano) placed in backscatter geometry (180°). All XRF detectors were used in combination with Xspress 3 pulse processors (Quantum Detectors, UK). Samples for tomographic μXRF measurements were inserted into Kapton capillaries and placed under a cryostream for analysis to reduce possible beam damage. Samples for 2D μXRF imaging were mounted on Kapton sticky tape with silicon adhesive (3 M™ Polyimide Film Tape 5413) stretched over a 3D printed ABS plastic frame and covered with Ultralene® Window Film, 4.0 μm thick (Cole-Parmer SamplePrep 3525).

Plant growth in controlled conditions

The seeds were sown in peat soil, and after 21 days, the seedlings were transferred to hydroponic culture. Each plant was placed in a 1 L polyethylene pot containing modified half-strength Hoagland's solution with the following composition: 3 mM KNO_3, 2 mM $Ca(NO_3)_2$, 1 mM $NH_4H_2PO_4$, 0.50 mM $MgSO_4$, 20 μM Fe(Na)- EDTA, 1 μM KCl, 25 μM H_3BO_3, 2 μM $MnSO_4$, 2 μM $ZnSO_4$, 0.1 μM $CuSO_4$ and 0.1 μM $(NH_4)_6Mo_7O_{24}$ (Hoagland and Arnon 1938) in milliQ- water (Millipore) buffered with 2 mM 2- morpholinoethanesulfonic acid, adjusted to pH 5.5 with KOH. Experiments were conducted in a growth chamber with a 16 h (day) photoperiod, day/night temperatures of 24/16 °C, irradiance of 300 μmol m^{-2} s^{-1} and 60%–65% relative humidity. After a pre- culture period of 7 days, plants of equal size were selected for treatment and exposed to 20 and 200 μM Zn (and 2000 μM only for the metallicolous population) supplied as $ZnSO_4$ (Sigma-Aldrich) and to 2.5 and 10 μM Tl supplied as $TlNO_3$ (Sigma-Aldrich) in a background solution with the same composition as the pre-culture solution (Figure S1). Plants were sampled at the beginning of the treatment and after 7 and 14 days of exposure. At each time point, six plants per treatment from each population were collected for root length and leaf area measurements to monitor growth increment at each interval (calculated by subtracting length or area values at the beginning of the treatment from those at the first and second intervals, as in Colzi et al. 2023). The length of the longest root of each plant was measured with a ruler, whereas

to measure leaf area, photographs from above were taken using a digital camera (Canon PowerShot SX100 IS) positioned 40 cm above the bottom of the pots. The software Fiji (Schindelin et al. 2012) was used for image analysis, and shoot area was expressed in cm^2. After biometric measurements, roots were gently washed with 1 mM EDTA at 4 °C for 15 min to desorb metals adhering to the cell wall, as in Körner et al. (1987). Roots and shoots were dried to constant weight at 40 °C for 72 h prior to elemental analysis.

Photosynthetic pigments and chlorophyll fluorescence analysis

At the end of the treatment, the chlorophyll content index was measured on the youngest fully expanded leaves using a Multi-Pigment-Meter (MPM-100, Opti-Sciences, USA). Stomatal conductance and chlorophyll fluorescence were determined using the LI-600 Porometer/Fluorometer (Li-Cor Inc., USA) at operational light intensity and the following parameters were recorded: stomatal conductance ($g_{s\ op}$), maximum quantum efficiency of the PSII in dark-adapted leaves ($F_V/F_{M\ op}$) and PSII efficiency in light-adapted leaves ($\varphi PSII_{op}$) (Maxwell and Johnson 2000). All measurements were taken from 9 to 12 a.m.

Elemental analysis of plant samples

The plant material was dried in a dehydrating oven at 60 °C for at least 48 h. It was then ground to a fine powder (< 200 µm) in an impact mill (IKA TubeMill 100 Control) and a 0.5 g subsamples were placed into custom XRF sample holders and covered with a 12 µm polypropylene thin film (Z-Spec Inc..) for XRF analysis. The XRF analysis of the powdered plant material was performed using an E-max instrument (Z-Spec Inc.). This instrumentation uses monochromatic X-ray fluorescence excitation at 17.48 keV to analyze elements from $Z = 13$ (Al) to $Z = 39$ (Y) on the K-lines and up to $Z = 92$ (U) on the L-lines, with optimum sensitivity for elements Cu–Se and Hg-Tl-Pb, and limits of detection ranging from 0.009–0.025 mg kg^{-1} (Zhang et al. 2026). Samples were analyzed for 30 s in plant mode. Quality controls included NIST SRM 1570a Trace elements in spinach leaves and NIST SRM 1573a Tomato leaves.

Data processing and statistical analyses

Data acquisition was carried out using a custom workflow (Garrevoet 2025), and the XRF data were processed with non-linear least squares fitting as implemented in PyMCA (Solé et al. 2007). Energy calibration was performed by measuring various thin film deposited foils with XRF emission lines that were well-spaced over the energy range (Micromatter Technologies Inc., Canada). For other elements, calibration was calculated using the foil measurement results in combination with parameters from *xraylib* (Schoonjans et al. 2011). The matrix used for modeling was hydrated plant material with the empirical formula $C_{7.3}O_{33}H_{59}N_{0.7}S_{0.8}$, a density of 0.8 g cm^{-3} and a thickness of 300 µm. This resulted in 32-bit.tiff files with pixel values corresponding to the area density of each element in µg cm^{-2} converted to µg g^{-1} values by: measured area density (µg cm^{-2})/(thickness of the layer (cm) × reference volume density (g cm^{-3})) for 2D measurements, and measured volume density (µg cm^{-3})/reference volume density (g cm^{-3}) for tomographic measurements. The figures were prepared in ImageJ (Schneider et al. 2012) by changing the lookup table (LUT) to 'Fire' and adjusting the pixel intensity range with the levels slider so that the background is scaled to black and the highest concentration values are scaled to the upper end of the LUT (nearly white). Concentration scale bars were added using the 'calibration' tool, along with length scales. All tomographic datasets were reconstructed using a maximum-likelihood expectation–maximization (MLEM) algorithm (Bruyant 2002).

A two-way ANOVA (statistical significance at $p < 0.05$) was performed to evaluate the effect of metal treatment on the two populations (metallicolous vs. non-metallicolous) and their interaction. Post hoc comparisons were carried out using the Tukey HSD test in GraphPad Prism 7 (GraphPad Software) after assessing data normality (assessed with the Shapiro–Wilk test).

Results

Distribution of thallium and zinc in *Anthyllis vulneraria* plant tissues

Spatial analysis of Tl distribution in roots of field-collected *A. vulneraria* subsp. *polyphylla* (metallicolous population) indicated marked enrichment in the epidermis (Fig. 1). Lower concentrations were observed in the outer layer of the cortical parenchyma, decreasing further toward the inner root structures, with depletion in the stele. Apart from the notably higher concentrations in the epidermis, and some enrichment in the intercellular areas of the cortex, Zn distribution in the root was much more homogeneous. As with Tl, depletion in the stele was also observed for Zn. In regions of highest accumulation, concentrations of both Tl and Zn exceeded 3000 µg g^{-1} d.w.

Epidermal accumulation of Tl was also observed in the petiole (Fig. 1), with most Tl deposited in the vacuoles. In collenchyma, enrichment was lower, with higher levels in the outer layers, whereas accumulation was also observed in the phloem of the central vascular tissue. For Zn, collenchyma was the primary site of localization, with significant accumulation in the epidermis as well. In contrast to Tl, where similar levels were found in the roots and petiole, the petiole showed reduced Zn concentrations compared to the

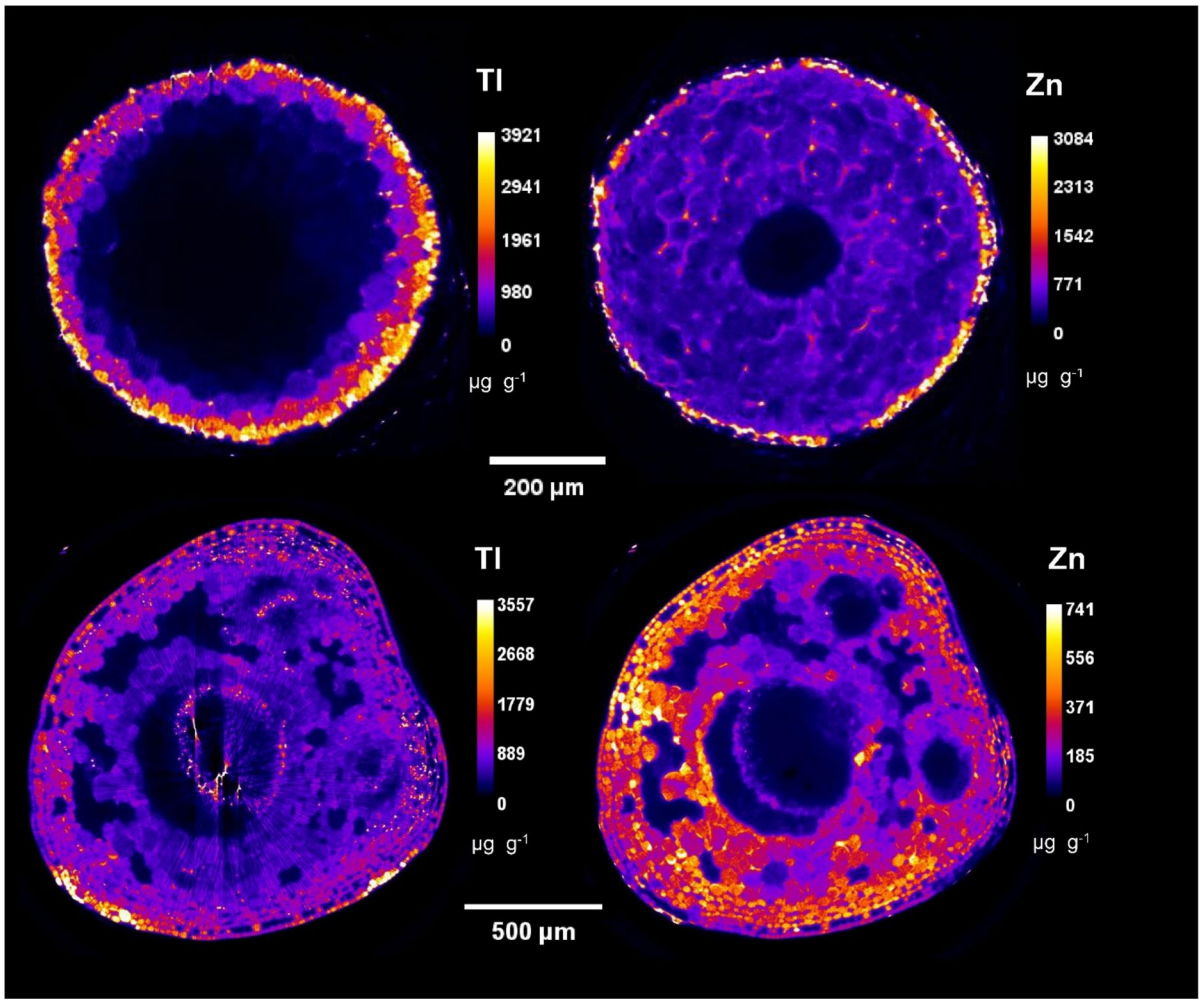


Fig. 1 Synchrotron-based µXRF elemental maps of Tl and Zn in root (upper part) and petiole (lower part) of *Anthyllis vulneraria* subsp. *polyphylla* from metallicolous population

roots. The distribution of Tl in *A. vulneraria* leaves was confined to the vasculature, primarily the central vein (Fig. 2). Accumulation was highest in the basal part of the leaf, with concentrations reaching nearly 2000 μg g^{-1}. Toward the apex, concentrations sharply decreased, whereas the epidermal tissue showed general depletion of Tl. Zinc was also primarily localized in the vasculature, however, concentrations were more uniformly distributed, with enrichment in the primary and secondary veins, as well as the central vein. Depletion in the epidermis was also observed for Zn.

In nodules, Tl exhibited the greatest enrichment in the cortical parenchyma, especially in the basal region (Fig. 3). In the epidermis, concentrations were considerably lower, with depletion in the central tissue. Zinc showed a more uniform localization, with enrichment in the epidermis, cortex, and central tissue containing a homogeneous population of bacteroids.

Growth and metal accumulation in metallicolous and non-metallicolous *Anthyllis vulneraria*

For both root length and increase in leaf area, a significant treatment × time interaction was found in the non-metallicolous plants (Table S1), where Zn exposure significantly reduced growth compared to controls (Fig. 4). In contrast, metallicolous plants showed no significant reduction in root growth in response to Zn, and, at the lowest concentration, the metal even promoted an increase in leaf area compared to controls, resulting in a significant treatment × time interaction. Similar results were observed with Tl treatment (Fig. 5, Table S2), with metal-induced

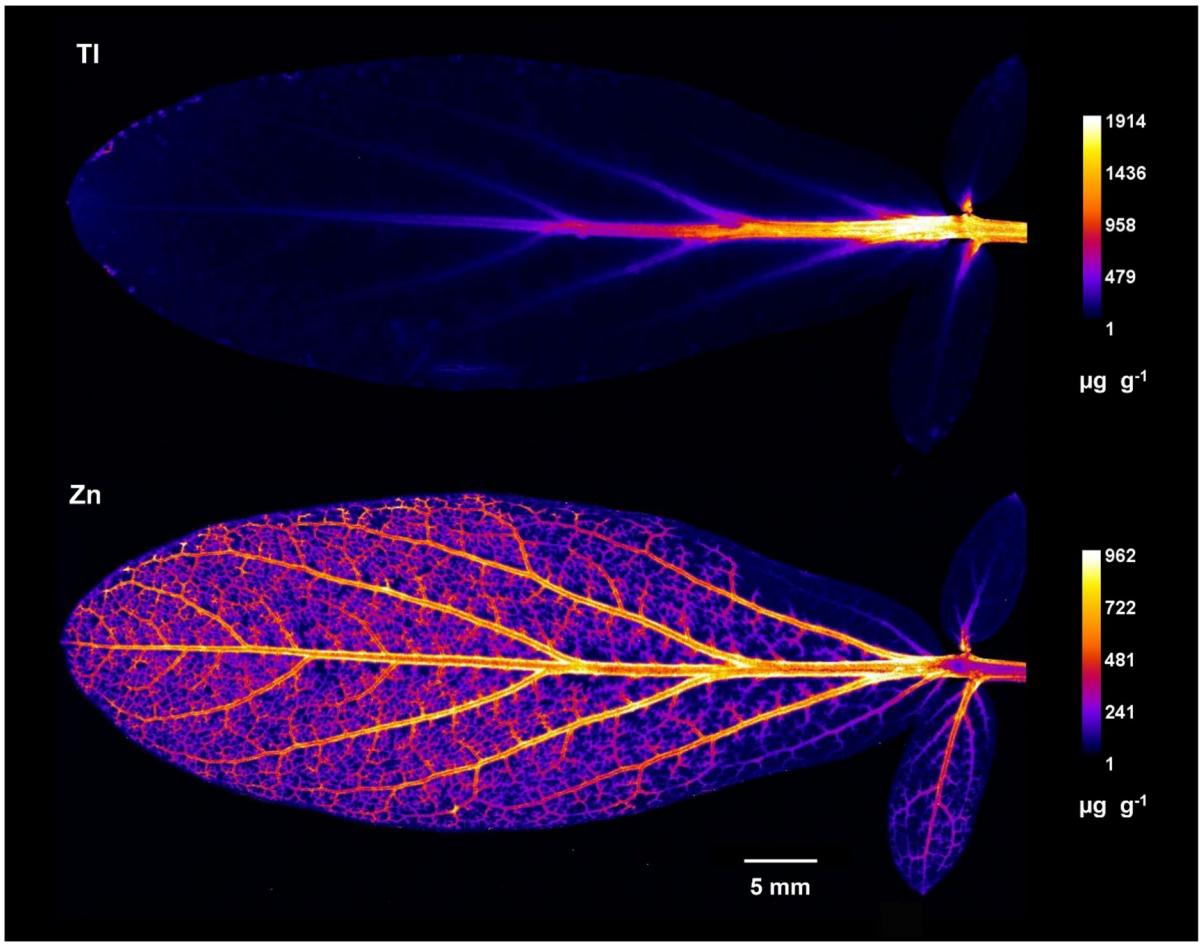


Fig. 2 Synchrotron-based μXRF elemental maps of Tl and Zn in *Anthyllis vulneraria* subsp. *polyphylla* leaf from metallicolous population

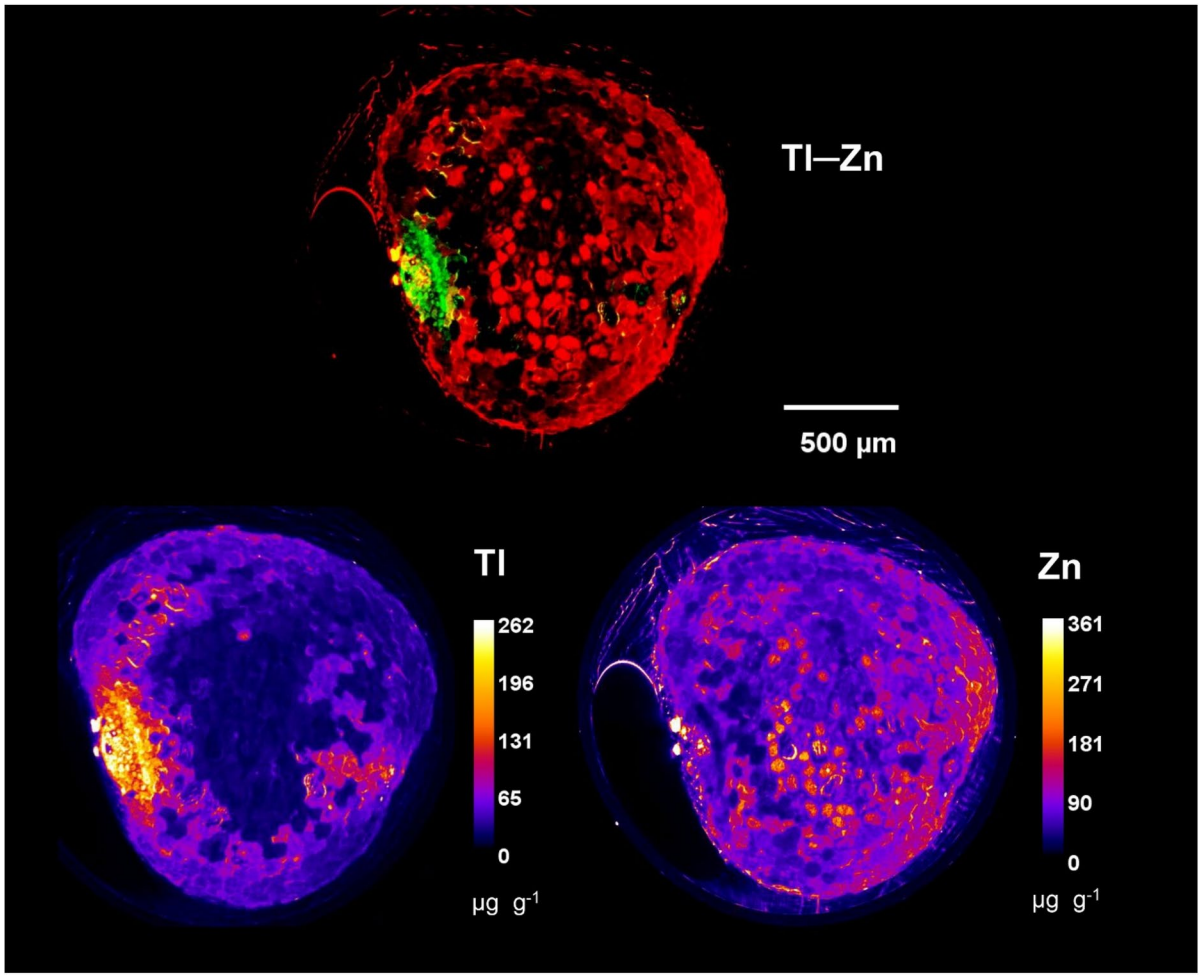


Fig. 3 Synchrotron-based µXRF elemental maps of Tl and Zn in root nodule of *Anthyllis vulneraria* subsp. *polyphylla* from metallicolous population

growth reductions in the non-metallicolous population and significant Tl-induced increases in leaf area increment in the metallicolous plants at the end of the exposure period.

Metal concentrations in roots and shoots, measured at the end of the exposure period, increased with rising metal concentrations in the root zone in both metallicolous and non-metallicolous populations (Fig. 6). Zinc concentrations in roots were significantly higher than in shoots for both populations, with higher concentrations in both roots and shoots of metallicolous plants (790 and 250 µg Zn g^{-1} d.w. in the latter), and a significant treatment × population interaction (Table S3). In response to 2000 µM Zn, shoots of the metallicolous population reached approximately 4000 µg Zn g^{-1} d.w., significantly lower than the roots (approximately 11,000 µg Zn g^{-1} d.w.). Conversely, exposure to higher concentrations of Tl resulted in similar concentrations in roots and shoots in both populations (approximately 600 and 880 µg Tl g^{-1} d.w. for non-metallicolous and metallicolous populations, respectively), whereas at the lower concentration, metal accumulation was higher in roots in the non-metallicolous population and higher in shoots in the metallicolous population. The latter value (approximately 300 µg Tl g^{-1} d.w.) was significantly higher than that of the non-metallicolous population (approximately 120 µg Tl g^{-1} d.w.), as indicated by the significant population × treatment interaction (Table S3).

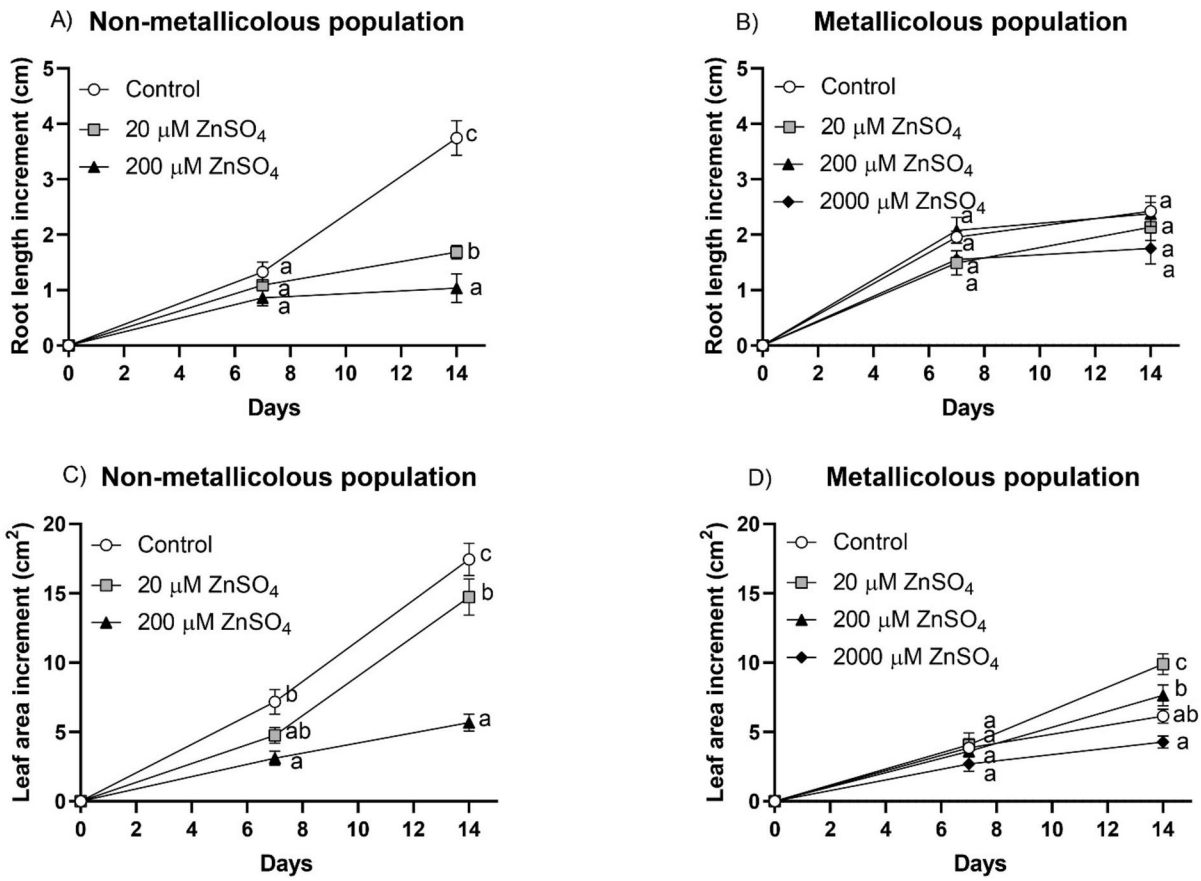


Fig. 4 Increase in: **A–B**) root length and **C–D**) leaf area of non-metallicolous and metallicolous populations of *Anthyllis vulneraria* subsp. *polyphylla* exposed to $ZnSO_4$ for 14 days. Increase was calculated by subtracting the values at the beginning of the treatment from those at the end. Values are means ± SE of 6 replicates. Letters next to the data points indicate significant differences among samples at each exposure time according to Tukey's test (at least $p < 0.05$)

Consequently, the shoot:root ratio was always below unity for Zn, with significant metal-induced decreases compared to control conditions in the non-metallicolous plants, while in the metallicolous plants the highest treatment resulted in an increase (Table 2). The population × treatment interaction was significant, despite similar values in the two groups of plants (Table S4). For Tl, the non-metallicolous plants had no differences among treatments, with values below or around unity. In contrast, the metallicolous plants showed a shoot:root ratio of around 3 at the lowest treatment, which decreased significantly to about one at the highest treatment. The interaction between population and treatment was significant, and the metallicolous plants had a significantly higher ratio compared to the non-metallicolous plants at 2.5 μM Tl.

Photosynthetic pigments and chlorophyll fluorescence analysis

Chlorophyll fluorescence parameters, stomatal conductance and chlorophyll content index were assessed at the end of the exposure period, following sufficient leaf development. The results for Zn and Tl are shown in Figs. 7 and 8. Under operational conditions, F_V/F_{Mop} values were significantly lower in plants exposed to 200 μM Zn in the non-metallicolous population and 2000 μM Zn in the metallicolous population, compared to the respective controls. Two-way

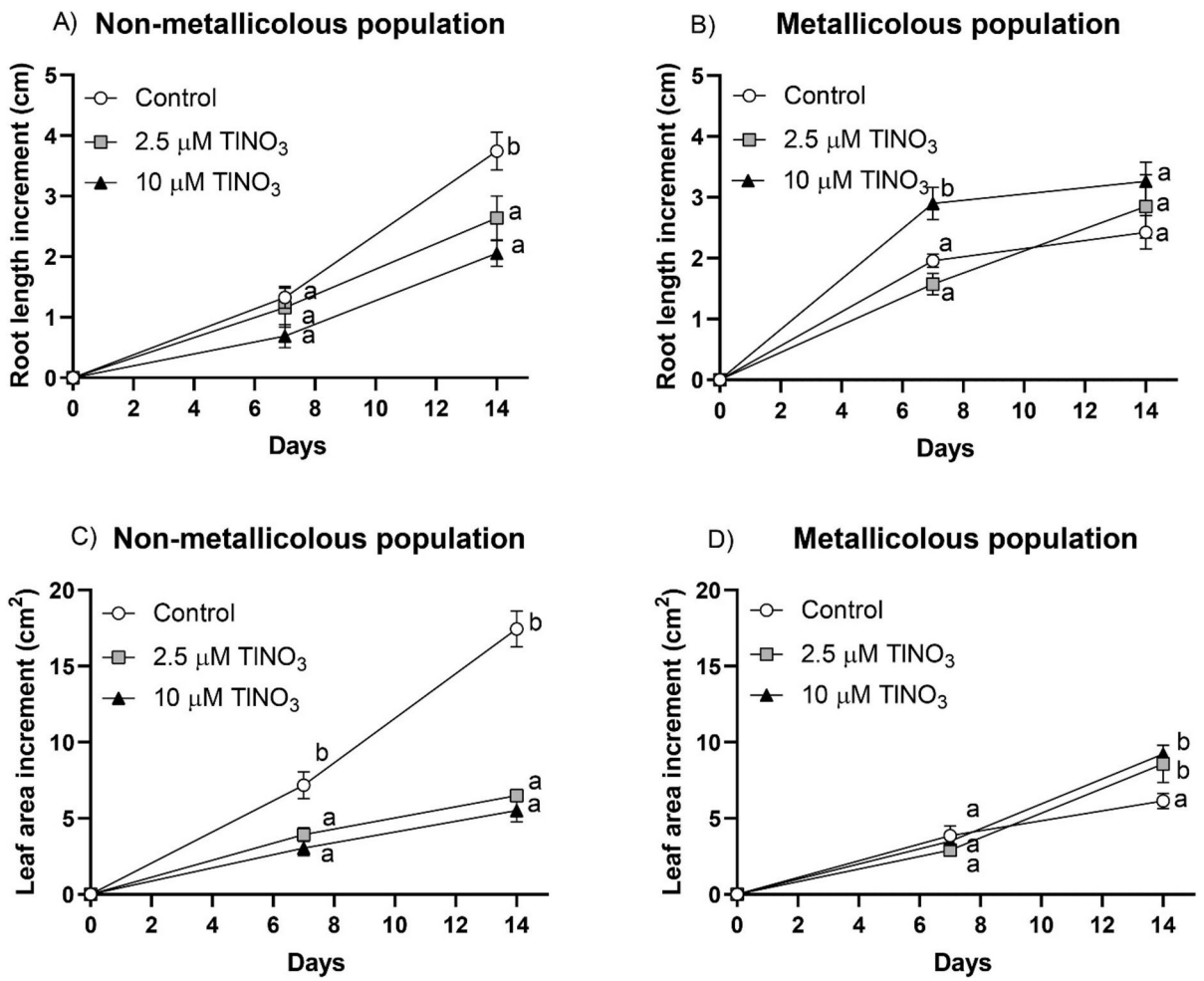


Fig. 5 Increase in: **A–B**) root length and **C–D**) leaf area of the non-metallicolous and metallicolous populations of *Anthyllis vulneraria* subsp. *polyphylla* exposed to $TlNO_3$ for 14 days. Increase was calculated by subtracting the values at the beginning of the treatment from those at the end. Values are means ± SE of 6 replicates. Letters next to the data points indicate significant differences among samples at each exposure time according to Tukey's test (at least $p < 0.05$)

ANOVA revealed a significant population × treatment interaction (Table S5). Values of $\varphi PSII_{op}$ and the chlorophyll content index showed similar results, with an additional Zn-induced decrease in the latter parameter at 200 μM also observed in the metallicolous plants. For stomatal conductance (g_{sop}), no significant population × treatment interaction was found, with the metal reducing this value only at 200 μM Zn in the non-metallicolous plants and at 2000 μM Zn in the metallicolous plants. For Tl treatment, all measured parameters were reduced at the highest Tl concentration in the non-metallicolous population, while only g_{sop} declined in the metallicolous population. Two-way ANOVA showed significant interaction effects only for $F_V/F_{M\ op}$ and the chlorophyll content index (Table S6).

Discussion

Tissue-level distribution of thallium and zinc in *Anthyllis vulneraria*

Despite the high shoot Tl and Zn concentrations in *vulneraria* subsp. *polyphylla*, the elemental sequestration in the root epidermis, observed for both Tl and

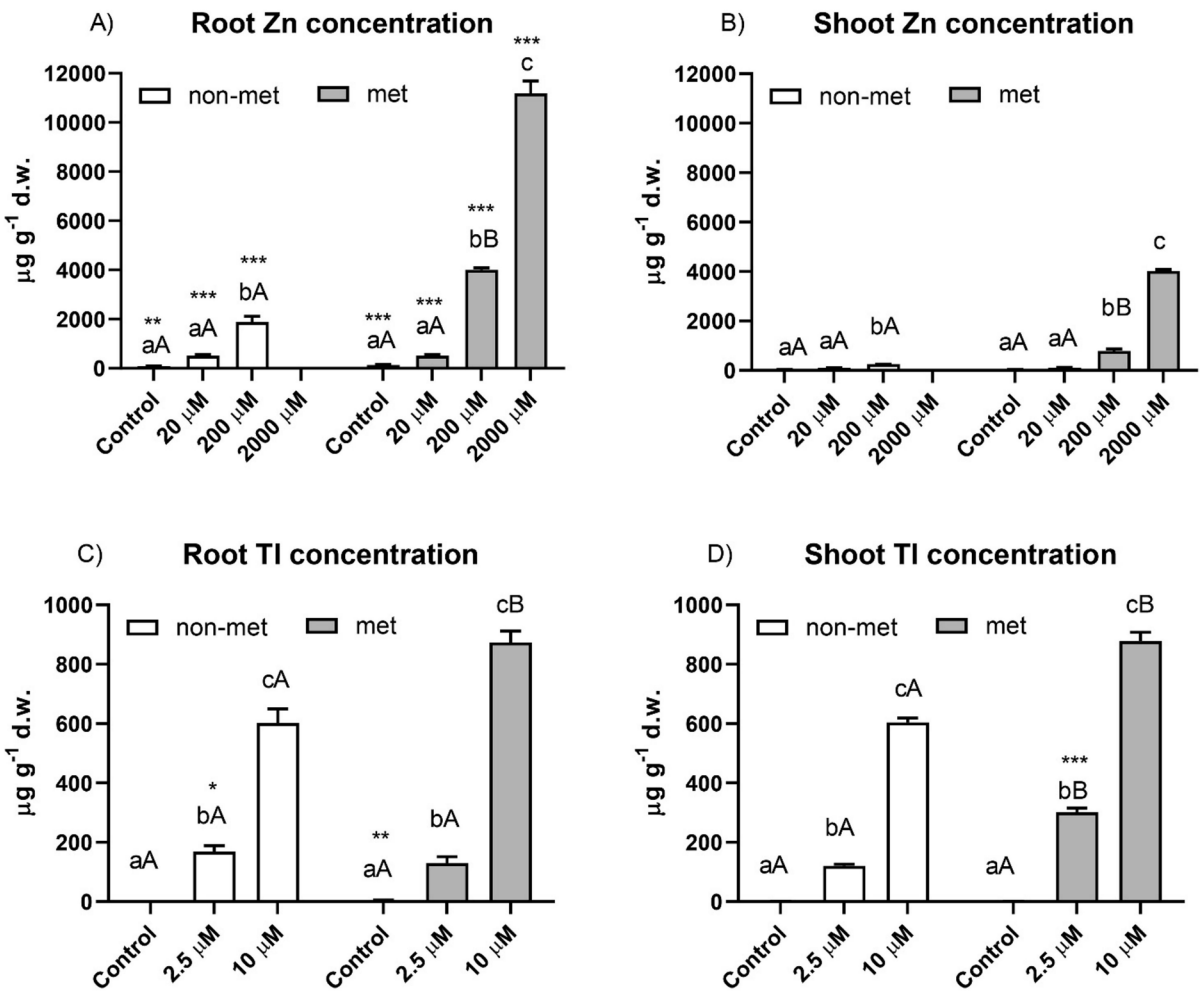


Fig. 6 Metal concentrations in non-metallicolous and metallicolous populations of *Anthyllis vulneraria* subsp. *polyphylla* exposed for 14 days to $ZnSO_4$: **A**) roots, **B**) shoots, and to $TlNO_3$: **C**) roots, **D**) shoots. Values are means ± SE of 6 replicates. Letters indicate significant differences among samples according to Tukey's test (at least $p < 0.05$), with capital letters for inter-population comparisons and lower-case letters for intra-population comparisons. Asterisks indicate the highest values between roots and shoots in intra-treatment comparisons according to the t-test (* $p < 0.05$, ** $p < 0.01$, *** $p < 0.001$)

Table 2 Shoot:root ratios of the metallicolous and non-metallicolous populations of *Anthyllis vulneraria* subsp. *polyphylla* exposed to $ZnSO_4$ and to $TlNO_3$ for 14 days. Values are means ± SE of 6 replicates. Letters indicate significant differences among samples according to Tukey's test (at least $p < 0.05$), with capital letters for inter-population comparisons and lower-case letters for intra-population comparisons and separately for Zn and Tl treatment

Population	Treatment	Control	1 st concentration	2nd concentration	3rd concentration
non-metallicolous	Zn	0.36 ± 0.03bB	0.21 ± 0.07aA	0.14 ± 0.04aA	
metallicolous	Zn	0.24 ± 0.02aA	0.21 ± 0.06aA	0.20 ± 0.05aA	0.36 ± 0.04b
non-metallicolous	Tl	0.78 ± 0.26aA	0.77 ± 0.24aA	1.04 ± 0.26aA	
metallicolous	Tl	0.33 ± 0.12aA	2.77 ± 0.77cB	1.02 ± 0.15bA	

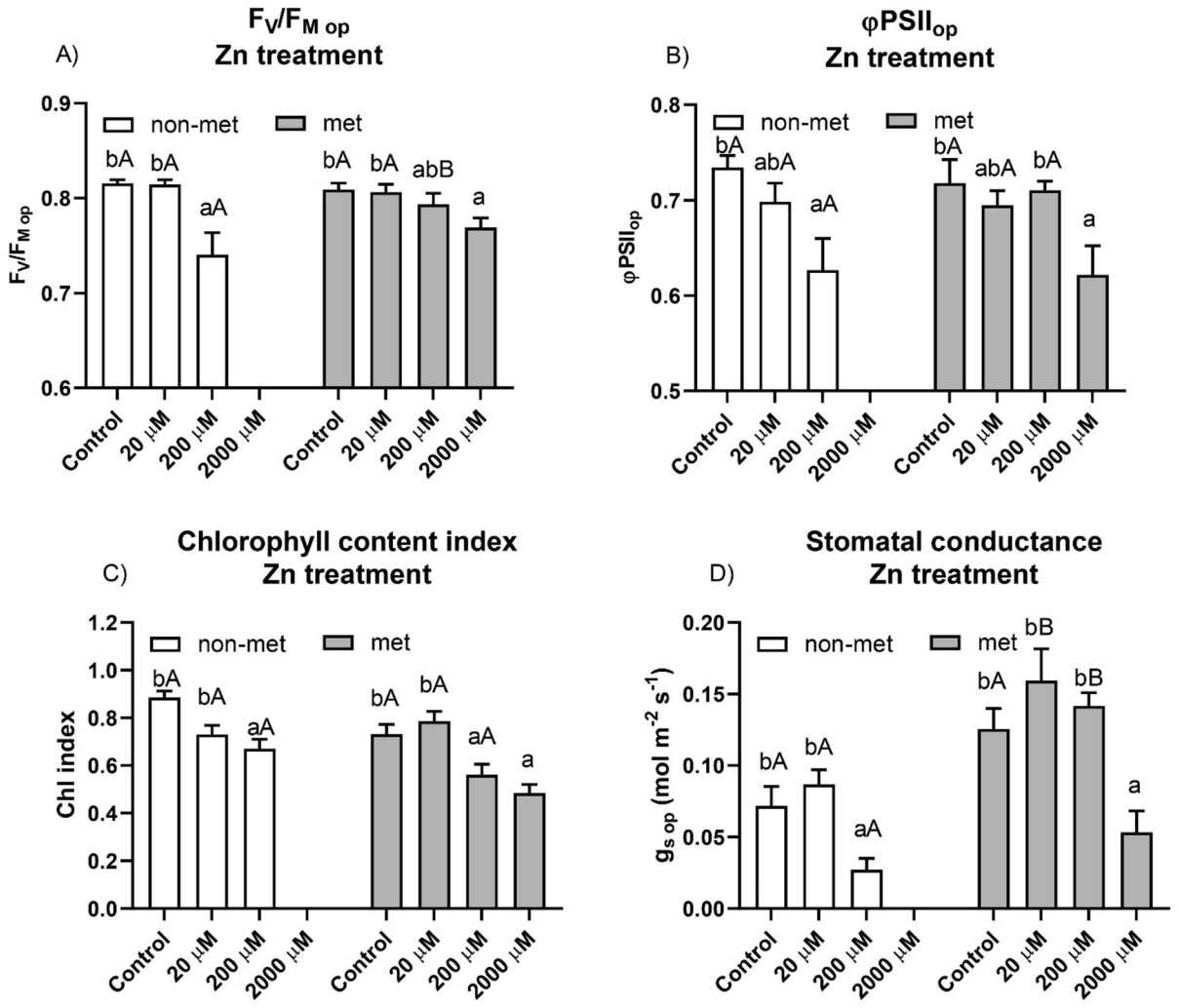


Fig. 7 Photosynthetic parameters in non-metallicolous and metallicolous populations of *Anthyllis vulneraria* subsp. *polyphylla* exposed for 14 days to $ZnSO_4$: **A**) $F_V/F_{M\ op}$, **B**) $\varphi PSII_{op}$, **C**) Chlorophyll index and **D**) $g_{s\ op}$. Values are means ± SE of 6 replicates. Letters indicate significant differences among samples according to Tukey's test (at least $p < 0.05$), with capital letters for inter-population comparison and lower-case letters for intra-population comparison

Zn, is generally a trait associated with non-hyperaccumulator species, with restricted translocation to the shoot (Xing et al. 2008), rather than with (hyper)accumulators. The same applies to the localization of Zn in the cortical apoplast, previously observed in *N. caerulescens* (White et al. 2002), although its significance for xylem loading has not been confirmed. Apart from the enrichment in the epidermis, also observed in *B. laevigata*, another Tl-hyperaccumulator (van der Ent et al. unpublished), Tl distribution in root tissues of *A. vulneraria* subsp. *polyphylla* largely corresponds to that observed in Tl (hyper)accumulators such as *Silene latifolia* (Regini et al. 2026) and *Viola tricolor* subsp. *macedonica* (Jakovljević et al. 2025b). In these species, Tl is localized in the root cortex and is restricted to the outer zone, indicating transient ion accumulation during radial transport. Although this could imply restricted root-to-shoot transport, as consistently seen in excluder species, depletion in the stele, observed for both Tl and Zn, might result from continuous transfer of Tl from the cortex and indicate efficient xylem loading.

Although restricted to discrete regions (probably associated with the distribution of transporters), high

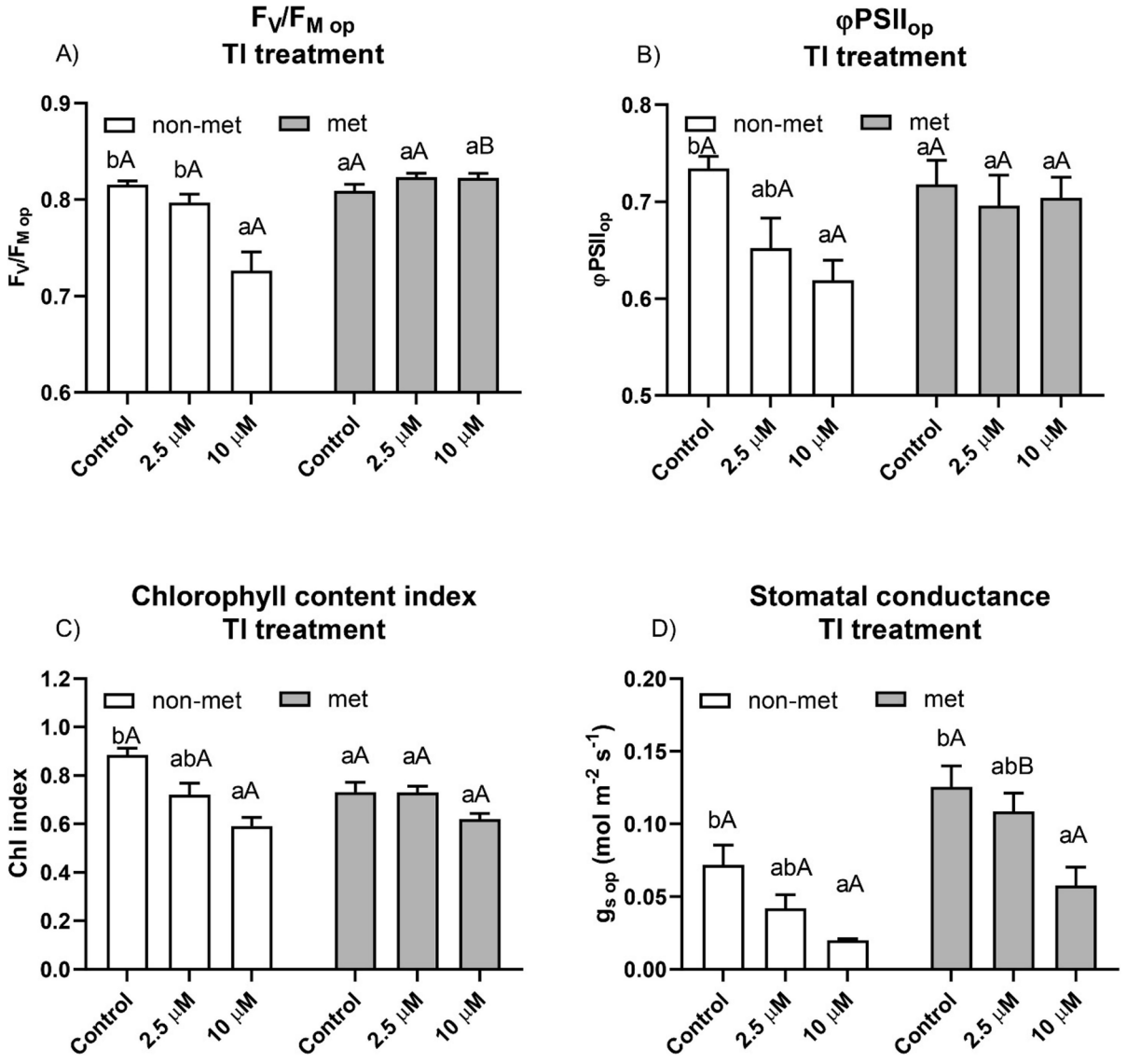


Fig. 8 Photosynthetic parameters in the non-metallicolous and metallicolous populations of *Anthyllis vulneraria* subsp. *polyphylla* exposed for 14 days to $TlNO_3$ with: **A**) $F_V/F_{M\ op}$, **B**) $\varphi PSII_{op}$, **C**) Chlorophyll index and **D**) $g_{s\ op}$. Values are means ± SE of 6 replicates. Letters indicate significant differences among samples according to Tukey's test (at least $p < 0.05$), capital for inter-population comparison and lower for intra-population comparison

Tl in the petiole of *A. vulneraria* subsp. *polyphylla* was predominantly sequestered in the epidermis. This has been previously observed in *B. laevigata* (Salinitro et al. 2024) and the Tl-hyperaccumulating accession of *S. latifolia* (Regini et al. 2026). Enrichment of both Tl and Zn in the vasculature suggests intensive translocation to the leaves, where they accumulated mainly in the central vein. In contrast to Tl, whose concentrations sharply decreased from the base toward the tip of the leaf, Zn was distributed homogeneously in the vasculature across the lamina. Vein-enrichment of Zn was also found in different accessions of *N. caerulescens*, where water-storage cells (or metal-storage cells; Leitenmaier and Küpper 2013), located close to the vascular bundles, represent the main deposits of Zn and act as an elemental source (Kozhevnikova et al. 2017). In non-accumulators this feature has not been observed (Kozhevnikova et al. 2014).

In *A. vulneraria* subsp. *polyphylla* nodules, Tl accumulates in the cortex, mainly in the senescent zone, suggesting elemental recycling, with some enrichment in the meristematic zone. Both zones are bacteria-free and distant from the zone of nitrogen fixation and from the zone where rhizobia are released into host cells and differentiate (Vasse et al. 1990). In contrast, Zn distribution was by far more uniform, with enrichment in the central zones, which are rich in bacteria. Besides Zn, the nodules also represent a sink for other essential elements, such as Fe and Cu, which were particularly enriched inside the *rhizobia*-infected cells, with differences in accumulation reflecting varying preferences of rhizobia for these elements (Abreu et al. 2017; Rodríguez-Haas et al. 2013).

Zinc and thallium tolerance and accumulation

Field-collected *A. vulneraria* subsp. *polyphylla* plants exhibited remarkably high Zn and Tl concentrations, exceeding both toxicity and hyperaccumulation thresholds (Kabata-Pendias and Pendias 2001; Reeves et al. 2018), with tissue and cellular localization displaying features similar to those in other hyperaccumulators. Nevertheless, experiments under controlled conditions remain the only clear-cut method for determining the actual levels of trace metal tolerance and accumulation in putative hyperaccumulator plants (van der Ent et al. 2024). Compared to a reference population from an uncontaminated soil in the same region, Zn and Tl differentially affected plant development in the two contrasting populations, with metal-induced growth reductions occurring mainly in non-metallicolous plants. The metallicolous population, on the other hand, had enhanced Zn and Tl tolerance, probably as an evolutionary response to the selective pressure exerted by long-term exposure to the high metal load of the mine spoil (Macnair 1993). Although specific adaptive tolerance to element excess has often been demonstrated by comparing metallicolous and non-metallicolous populations under controlled conditions (e.g., Arnetoli et al. 2008; Colzi et al. 2014; Schat and Vooijs 1997), to the best of our knowledge, this is the first report for a facultative metallophyte in the Fabaceae family. All previous studies on *A. vulneraria* subspecies concern *A. vulneraria* reference populations and are limited to observations on field-collected plants (Sujkowska-Rybkowska et al. 2020, 2023), transplanting experiments (Mahieu et al. 2013) or hydroponic trials comparing different subspecies rather than the same one (Soussou et al. 2013). For other leguminous facultative metallophytes, except for *A. vulneraria*, there is only a single hydroponic study available on *Dorycnium pentaphyllum* subjected to Zn and Cd (Lefèvre et al. 2009). The lack of a non- metallicolous population in this study, however, does not allow a comparative analysis.

Across treatments, higher concentrations of Zn and Tl in the metallicolous accession of *A. vulneraria* subsp. *polyphylla* were the dominant response, with restricted root uptake not representing the adaptation mechanism to the excessive concentrations of Zn and Tl present at the Cave del Predil site. There were substantial differences in the allocation of the two elements between roots and shoots, allowing a clear definition of this species within the metallophyte categories of accumulator or excluder (Baker 1981). As preliminarily observed in a pot experiment with only metallicolous plants (Fellet et al. 2014), the higher Zn concentrations in roots than in shoots, resulting in a concentration ratio below unity, indicate that *A. vulneraria* subsp. *polyphylla* cannot be considered as a genuine hyperaccumulator. This confirms the pattern found in previous studies in other *A. vulneraria* subspecies (Soussou et al. 2013), although complementary studies on *A. vulneraria* (non-metallicolous) plants were not included. This study therefore indicates that *A. vulneraria* subsp. *polyphylla* has an excluder strategy and cannot be considered a true hyperaccumulator, despite the fact that in field-collected plants at Cave del Predil and hydroponically grown plants treated with 2000 µM reached or exceeded the hyperaccumulation threshold for Zn (Krämer 2010; van der Ent et al. 2024). Thus, the remarkable shoot metal concentrations appear to result from exclusion mechanisms combined with enhanced internal tolerance for Zn, compared to *A. vulneraria* (non-metallicolous) populations.

Compared to Zn, a different scenario was observed for Tl. The metallicolous accession predominantly accumulated Tl in shoots under lower Tl treatment, while the opposite pattern occurred in the non-metallicolous population. Therefore, as the aboveground tissues appeared to be the main sink for Tl allocation, reaching levels above the hyperaccumulation threshold, *A. vulneraria* subsp. *polyphylla* can be classified among the few genuine Tl hyperaccumulating plants

recorded so far (Reeves et al. 2018). Furthermore, it represents the first legume identified as a Tl hyperaccumulator under controlled conditions. The higher treatment, however, reduced the differences in root and shoot Tl concentrations and lowered the shoot:root ratio, possibly because the hyperaccumulation capacity of this species could not reach the extreme levels observed in other plants in hydroponics (Regini et al 2024; Salinitro et al. 2024) or in field-collected samples (Escarrè et al. 2011; Jakovljević et al. 2025a).

Metal-induced changes in plant growth were associated with similar changes in gas exchange and photosynthetic efficiency in both populations, indicating causal links. In the non-metallicolous population, metal-induced stomatal limitations and reductions in PSII activity likely contributed to reduced growth in treated plants with increasing Zn and Tl concentrations in the root zone. This is probably due to the known negative impact of excess trace metals on the photosynthetic apparatus, pigment content, and stomatal conductance (Chang et al. 2024; Jagota et al. 2026; Mazur et al. 2016; Yruela 2013). Conversely, the metallicolous population showed general stability in photosynthetic parameters across almost all concentrations tested, with some differences between the two metals.

In the case of Zn, at 200 µM, the stomatal functioning and photosynthetic apparatus in metallicolous plants remained stable, with values comparable to those of control plants. This stability could be partly attributed to the significant decrease in chlorophyll content, mechanism already known to provide photoprotection by reducing the size of the light-harvesting antennae under Zn excess, as reported by Moustakas et al. (2024). At the higher concentration of 2000 µM, at which the non-metallicolous *A. vulneraria* plants were unable to grow, the further decrease in chlorophyll content in metallicolous plants may instead indicate emerging metal toxicity. This is confirmed by the decrease in all other photosynthetic parameters, as generally shown for Zn stress (Jagota et al. 2026). Under the experimental conditions used, this incipient depression of photosynthetic activity was not yet accompanied by a significant decrease in plant growth, although the beginning of a decreasing trend in leaf area increment at this concentration in metallicolous plants was already evident.

Conversely, at all Tl concentrations, the metallicolous population maintained stable photosynthetic activity, probably due to the continued efficiency of detoxification/hyperaccumulation mechanisms protecting the photosynthetic apparatus, as suggested in *S. latifolia* (Regini et al. 2024). However, a significant decrease in stomatal conductance was observed at the highest Tl treatment. Stomatal closure in the presence of Tl has already been reported (Domínguez et al. 2011; Mazur et al. 2016) and, in the metallicolous population, this could represent the onset of initial responses to limit Tl transpirational allocation to the shoot. This would be consistent with the previously hypothesized inability of this plant to reach extremely toxic shoot metal concentrations and would explain the observed decrease in the shoot:root ratio.

Conclusions

Spatial analysis of Zn and Tl distribution in field-collected *A. vulneraria* subsp. *polyphylla* from Cave del Predil revealed features typical of metal hyperaccumulators, such as preferential accumulation in the petiole epidermis, while others, such as metal enrichment in the root epidermis, were less common. Comparative study under controlled conditions suggested selection for enhanced Zn and Tl tolerance in the metallicolous population compared to the non-metallicolous population. Despite metal concentrations above threshold levels in both field-collected and hydroponically grown plants, hyperaccumulation was observed only for Tl, whereas exclusion mechanisms coupled with high internal tolerance were found for Zn. The comparative analyses of metallicolous and non-metallicolous populations of *A. vulneraria* subsp. *polyphylla* elucidate the tendency for Tl and Zn accumulation, confirming the species as a genuine Tl hyperaccumulator.

Acknowledgements We acknowledge DESY (Hamburg, Germany), a member of the Helmholtz Association HGF, for the provision of experimental facilities. Parts of this research were carried out at PETRA III. Data was collected using beamline P06 operated/provided by DESY Photon Science. Beamtime was allocated for proposal I-20250020 EC. This research was supported in part through the Maxwell computational resources operated at Deutsches Elektronen-Synchrotron DESY, Hamburg, Germany. We would like to thank Gerald Falkenberg and Jan Garrevoet for assistance in using beamline P06.

Author contributions CG and AvdE conceived and planned the study. GR, MD, PCV, IC and NB conducted the

hydroponics dosing experiment. LP and LM collected and analysed the field material. GR, CG, MD, KJ, DB and AvdE conducted the synchrotron experiment. DB performed the fitting of the XRF data and KJ processed the data for figure preparation. KJ and AvdE designed the figures. CG, KJ and AvdE evaluated and interpreted the data. KJ, CG and AvdE drafted the manuscript. All authors provided critical feedback and helped shape the research, analysis and manuscript.

Funding The authors acknowledge the support of National Biodiversity Future Centre to the University of Florence, Department of Biology, funded by the Italian Ministry of University and Research, PNRR, Missione 4 Componente 2, "Dalla ricerca all'impresa", Investimento 1.4, Project CN00000033. Authors are grateful to Ignazio Giarrizzo for his contribution in the experimental work of the hydroponic experiment. KJ acknowledges the support of Ministry of Science, Technological Development and Innovation of the Republic of Serbia (Grant Number 451–03-33/2026–03/200007).

Data Availability The data that support this study will be shared upon reasonable request to the corresponding author.

Declarations

Conflict of interest The authors declare no conflicts of interest relevant to the content of this manuscript.

References

Abreu I, Saez A, Castro-Rodriguez R, Escudero V, Rodriguez-Haas B, Senovilla M, Larue C, Grolimund D, Tejada-Jimenez M, Imperial J, González-Guerrero M (2017) *Medicago truncatula* zinc-iron permease6 provides zinc to rhizobia-infected nodule cells. Plant Cell Environ 40:2706–2719. https://doi.org/10.1111/pce.13035

Arnetoli M, Vooijs R, Gonnelli C, Gabbrielli R, Verkleij JAC, Schat H (2008) High-level Zn and Cd tolerance in *Silene paradoxa* L. from a moderately Cd- and Zn-contaminated copper mine tailing. Environ Pollut 156:380–386. https://doi.org/10.1016/j.envpol.2008.01.044

Bačeva K, Stafilov T, Šajn R, Tănăselia C, Makreski P (2014) Distribution of chemical elements in soils and stream sediments in the area of abandoned Sb-As-Tl Allchar mine, Republic of Macedonia. Environ Res 133:7–89. https://doi.org/10.1016/j.envres.2014.03.045

Baker AJM (1981) Accumulators and excluders—strategies in the response of plants to heavy metals. J Plant Nutr 3:643–654. https://doi.org/10.1080/01904168109362867

Boesenberg U, Ryan CG, Kirkham R, Siddons DP, Alfeld M, Garrevoet J, Núñez T, Claussen T, Kracht T, Falkenberg G (2016) Fast X-ray microfluorescence imaging with submicrometer-resolution integrating a Maia detector at beamline P06 at PETRA III. J Synchrotron Radiat 23:1550–1560. https://doi.org/10.1107/S1600577516015289

Brooks RR (1979) Indicator plants for mineral prospecting—a critique. J Geochem Explor 12:67–78. https://doi.org/10.1016/0375-6742(79)90064-5

Brooks RR, Yang XH (1984) Elemental levels and relationships in the endemic serpentine flora of the Great Dyke, Zimbabwe and their significance as controlling factors for the flora. Taxon 33:392–399. https://doi.org/10.1002/j.1996-8175.1984.tb03892.x

Brooks RR, McCleave JA, Malaisse F (1977) Copper and cobalt in African species of *Crotalaria* L. Proc R Soc Lond B Biol Sci 197:231–236. https://doi.org/10.1098/rspb.1977.0067

Bruyant PP (2002) Analytic and iterative reconstruction algorithms in SPECT. J Nucl Med 43:1343–1358

Chang HF, Tseng SC, Tang MT, Hsiao SS, Lee DC, Wang SL, Yeh KC (2024) Physiology and molecular basis of thallium toxicity and accumulation in *Arabidopsis thaliana*. Ecotoxicol Environ Saf 276:116290. https://doi.org/10.1016/j.ecoenv.2024.116290

Colzi I, Rocchi S, Rangoni M, Del Bubba M, Gonnelli C (2014) Specificity of metal tolerance and use of excluder metallophytes for the phytostabilization of metal polluted soils: the case of *Silene paradoxa* L. Environ Sci Pollut Res 21:10960–10969. https://doi.org/10.1007/s11356-014-3045-y

Colzi I, Gonnelli C, Bettarini I, Selvi F (2023) Polyploidy affects responses to Nickel in Ni-hyperaccumulating plants: evidence from the model species *Odontarrhena bertolonii* (Brassicaceae). Environ Exp Bot 213:105403. https://doi.org/10.1016/j.envexpbot.2023.105403

Dilshara P, Ratnayake N, Abeysinghe B, Premasiri R, Dushyantha N, Senarath S, Ratnayake AS, Batapola N (2024) Soil-to-resource approach to assess the Ni hyperaccumulating potential of native plant species for phytomining at Ginigalpelessa serpentinite deposit, Sri Lanka. Arabian J Geosci 17(3):90. https://doi.org/10.1007/s12517-024-11890-y

Domínguez MT, Marañón T, Murillo JM, Redondo-Gómez S (2011) Response of Holm oak (*Quercus ilex* subsp. *ballota*) and mastic shrub (*Pistacia lentiscus* L.) seedlings to high concentrations of Cd and Tl in the rhizosphere. Chemosphere 83(8):1166–1174. https://doi.org/10.1016/j.chemosphere.2011.01.002

Escarré J, Lefèbvre C, Raboyeau S, Dossantos A, Gruber W, Cleyet Marel JC, Frérot H, Noret N, Mahieu S, Collin C, van Oort F (2011) Heavy metal concentration survey in soils and plants of the Les Malines mining district (Southern France): implications for soil restoration. Water Air Soil Poll 216(1):485–504. https://doi.org/10.1007/s11270-010-0547-1

Farago ME, Clark AJ, Pitt MJ (1977) Plants which accumulate metals. Part I. The metal content of three Australian plants growing over mineralised sites. Inorg Chim Acta 24:53–56. https://doi.org/10.1016/S0020-1693(00)93850-7

Fellet G, Pošćić F, Casolo V, Marchiol L (2012) Metallophytes and thallium hyperaccumulation at the former Raibl lead/zinc mining site (Julian Alps, Italy). Plant Biosyst 146(4):1023–1036. https://doi.org/10.1080/11263504.2012.703250

Fellet G, Marmiroli M, Marchiol L (2014) Elements uptake by metal accumulator species grown on mine tailings amended with three types of biochar. Sci Total Environ 468:598–608. https://doi.org/10.1016/j.scitotenv.2013.08.072

Garrevoet J (2025) A framework for data processing used at the hard X-ray Micro/Nano Probe at PETRA III based on micro-services. J Phys: Conf Ser 3010:012136. https://doi.org/10.1088/1742-6596/3010/1/012136

Grison CM, Mazel M, Sellini A, Escande V, Biton J, Grison C (2015) The leguminous species *Anthyllis vulneraria* as a Zn-hyperaccumulator and eco-Zn catalyst resources. Environ Sci Pollut Res 22(8):5667–5676. https://doi.org/10.1007/s11356-014-3605-1

Hoagland DR, Arnon DI (1938) The water-culture method for growing plants without soil. Calif Agric Exp Stat Circ 347:1–39

Jagota N, Singh T, Sharma A, Chhabra R (2026) Deciphering cues of zinc toxicity and tolerance in plants: a comprehensive review. Acta Physiol Plant 48:9. https://doi.org/10.1007/s11738-025-03878-2

Jakovljević K, Bačeva Andonovska K, Salinitro M, Mišljenović T, van der Ent A (2025a) Biogeochemical survey of the Allchar (North Macedonia) arsenic-thallium ore body: a focus on hyperaccumulator plants. Plant Soil 513:1317–1331. https://doi.org/10.1007/s11104-025-07252-6

Jakovljević K, Salinitro M, Bačeva Andonovska K, Mišljenović T, Brueckner D, van der Ent A (2025b) Surviving Allchar: arsenic and thallium tolerance and distribution in *Viola* metallophytes. Ann Bot 136:1515–1524. https://doi.org/10.1093/aob/mcaf166

Kabata-Pendias A, Pendias H (2001) Trace elements in soils and plant. CRC Press, Boca Raton

Karbowska B (2016) Presence of thallium in the environment: sources of contaminations, distribution and monitoring methods. Environ Monit Assess 188:640. https://doi.org/10.1007/s10661-016-5647-y

Kazantzis G (2000) Thallium in the environment and health effects. Environ Geochem Health 22(4):275–280. https://doi.org/10.1023/A:1006791514080

Körner LE, Møller LM, Jensén P (1987) Effects of Ca^{2+} and other divalent cations on uptake of Ni^{2+} by excised barley roots. Physiol Plant 71:49–54. https://doi.org/10.1111/j.1399-3054.1987.tb04615.x

Kozhevnikova AD, Erlikh NT, Zhukovskaya NV, Obroucheva NV, Ivanov VB, Seregin IV (2014) Nickel and zinc accumulation, distribution and effects on ruderal plants *Lepidium ruderale* and *Capsella bursa-pastoris*. Acta Physiol Plant 36:3291–3305. https://doi.org/10.1007/s11738-014-1697-3

Kozhevnikova AD, Seregin I, Gosti F, Schat H (2017) Zinc accumulation and distribution over tissues in *Noccaea caerulescens* in nature and in hydroponics: a comparison. Plant Soil 411(1–2):5–16. https://doi.org/10.1007/s11104-016-3116-6

Kozhevnikova AD, Seregin IV, Aarts MG, Schat H (2020) Intra-specific variation in zinc, cadmium and nickel hypertolerance and hyperaccumulation capacities in *Noccaea caerulescens*. Plant Soil 452(1):479–498. https://doi.org/10.1007/s11104-020-04572-7

Krämer U (2010) Metal hyperaccumulation in plants. Annu Rev Plant Biol 61(1):517–534. https://doi.org/10.1146/annurev-arplant-042809-112156

Leblanc M, Petit D, Deram A, Robinson BH, Brooks RR (1999) The phytomining and environmental significance of hyperaccumulation of thallium by *Iberis intermedia* from southern France. Econ Geol 94(1):109–113. https://doi.org/10.2113/gsecongeo.94.1.109

Lefèvre I, Marchal G, Corréal E, Zanuzzi A, Lutts S (2009) Variation in response to heavy metals during vegetative growth in *Dorycnium pentaphyllum* Scop. Plant Growth Regul 59:1–11. https://doi.org/10.1007/s10725-009-9382-z

Leitenmaier B, Küpper H (2013) Compartmentation and complexation of metals in hyperaccumulator plants. Front Plant Sci 4:374. https://doi.org/10.3389/fpls.2013.00374

Li S, Qin M, Jiang L, Niu X, Wang Z, Xue W, Zhou Y, Kabir SF, Du H (2026) Tissue-specific thallium toxicity in the intestine and body wall of earthworms evaluated using a multi-biomarker approach. Ecotoxicology 35(5):99. https://doi.org/10.1007/s10646-026-03082-z

Liu J, Luo X, Sun Y, Tsang DC, Qi J, Zhang W, Li N, Yin M, Wang J, Lippold H, Chen Y (2019) Thallium pollution in China and removal technologies for waters: A review. Environ Int 126:771–790. https://doi.org/10.1016/j.envint.2019.01.076

Liu J, Huang Y, Liu Y, Jiang S, Zhang Q, Li P, Lin K, Zeng X, Hu H, Cao Y, Xiong X (2024) Increased atmospheric thallium threats to populated areas: a mini review. J Hazard Mater 480:135681. https://doi.org/10.1016/j.jhazmat.2024.135681

Macnair MR (1993) The genetics of metal tolerance in vascular plants. New Phytol 124:541–559. https://doi.org/10.1111/j.1469-8137.1993.tb03846.x

Mahieu S, Frérot H, Vidal C, Galiana A, Heulin K, Maure L, Brunel B, Lefèbvre C, Escarré J, Cleyet-Marel JC (2011) *Anthyllis vulneraria*/*Mesorhizobium metallidurans*, an efficient symbiotic nitrogen fixing association able to grow in mine tailings highly contaminated by Zn. Pb and Cd Plant Soil 342(1):405–417. https://doi.org/10.1007/s11104-010-0705-7

Mahieu S, Soussou S, Cleyet-Marel JC, Brunel B, Mauré L, Lefèbvre C, Escarré J (2013) Local adaptation of metallicolous and non-metallicolous *Anthyllis vulneraria* populations: their utilization in soil restoration. Restor Ecol 21:551–559. https://doi.org/10.1111/j.1526-100X.2012.00927.x

Maxwell K, Johnson GN (2000) Chlorophyll fluorescence - a practical guide. J Exp Bot 51(345):659–668. https://doi.org/10.1093/jexbot/51.345.659

Mazur R, Sadowska M, Kowalewska Ł, Abratowska A, Kalaji HM, Mostowska A, Garstka M, Krasnodębska-Ostręga B (2016) Overlapping toxic effect of long term thallium exposure on white mustard (*Sinapis alba* L.) photosynthetic activity. BMC Plant Biol 16:191. https://doi.org/10.1186/s12870-016-0883-4

Migaszewski ZM, Gałuszka A (2021) Abundance and fate of thallium and its stable isotopes in the environment. Rev Environ Sci Biotechnol 20:5–30. https://doi.org/10.1007/s11157-020-09564-8

Moustakas M, Dobrikova A, Sperdouli I, Hanć A, Moustaka J, Adamakis ID, Apostolova E (2024) Photosystem II tolerance to excess zinc exposure and high light stress in *Salvia sclarea* L. Agronomy 14:589. https://doi.org/10.3390/agronomy1403058

Ostrander CM, Shu Y, Nielsen SG, Dellwig O, Bluszstajn J, Schulz-Vogt HN, Hubner V, Hansel CM (2024)

Anthropogenic forcing of the Baltic Sea thallium cycle. Environ Sci Technol 58(19):8510–8517. https://doi.org/10.1021/acs.est.4c01487

Peter AJ, Viraraghavan T (2005) Thallium: a review of public health and environmental concerns. Environ Int 31(4):493–501. https://doi.org/10.1016/j.envint.2004.09.003

Pošćić F, Marchiol L, Schat H (2013) Hyperaccumulation of thallium is population-specific and uncorrelated with caesium accumulation in the thallium hyperaccumulator, *Biscutella laevigata*. Plant Soil 365:81–91. https://doi.org/10.1007/s11104-012-1384-3

Pošćić F, Fellet G, Vischi M, Casolo V, Schat H, Marchiol L (2015) Variation in heavy metal accumulation and genetic diversity at a regional scale among metallicolous and non-metallicolous populations of the facultative metallophyte *Biscutella laevigata* subsp. *laevigata*. Int J Phytoremediation 17:464–475. https://doi.org/10.1080/15226514.2014.922921

Ralph L, Twiss MR (2002) Comparative toxicity of thallium (I), thallium (III), and cadmium (II) to the unicellular alga *Chlorella* isolated from Lake Erie. Bull Environ Contam Toxicol 68:261. https://doi.org/10.1007/s00128-001-0247-z

Reeves RD, Brooks RR (1983) Hyperaccumulation of lead and zinc by two metallophytes from mining areas of Central Europe. Environ Pollut 31:277–285. https://doi.org/10.1016/0143-1471(83)90064-8

Reeves RD, Schwartz C, Morel JL, Edmondson J (2001) Distribution and metal-accumulating behavior of *Thlaspi caerulescens* and associated metallophytes in France. Int J Phytoremediation 3:145–172. https://doi.org/10.1080/15226510108500054

Reeves RD, Baker AJM, Jaffré T, Erskine PD, Echevarria G, van der Ent A (2018) A global database for hyperaccumulator plants of metal and metalloid trace elements. New Phytol 218:407–411. https://www.jstor.org/stable/90019919

Regini G, Bettarini I, Dainelli M, Chiavacci B, Colzi I, Selvi F, van der Ent A, Gonnelli C (2024) Highly distinctive population-specific thallium hyper-tolerance and hyperaccumulation in *Silene latifolia*. Environ Exp Bot 228:106005. https://doi.org/10.1016/j.envexpbot.2024.106005

Regini G, Jakovljević K, Dainelli M, Brueckner D, Gonnelli C, van der Ent A (2026) Cellular-level imaging reveals distinct thallium detoxification strategies in *Silene latifolia* accessions. Environ Exp Bot 28:106340. https://doi.org/10.1016/j.envexpbot.2026.106340

Richau KH, Schat H (2009) Intraspecific variation of nickel and zinc accumulation and tolerance in the hyperaccumulator *Thlaspi caerulescens*. Plant Soil 314:253–262. https://doi.org/10.1007/s11104-008-9724-z

Rodríguez-Haas B, Finney L, Vogt S, González-Melendi P, Imperial J, González-Guerrero M (2013) Iron distribution through the developmental stages of *Medicago truncatula* nodules. Metallomics 5:1247–1253. https://doi.org/10.1039/c3mt00060e

Salinitro M, Isnard S, Brueckner D, Spiers KM, Aarts MG, Corzo Remigio A, van der Ent A (2024) Uncovering the physiology and distribution of thallium in Tl- hyperaccumulating and Tl-sensitive populations of *Biscutella laevigata* L. Ann Bot 134:803–814. https://doi.org/10.1093/aob/mcae115

Schat H, Vooijs R (1997) Multiple tolerance and co-tolerance to heavy metals in *Silene vulgaris*: a co-segregation analysis. New Phytol 136:489–496. https://doi.org/10.1046/j.1469-8137.1997.00756.x

Schindelin J, Arganda-Carreras I, Frise E, Kaynig V, Longair M, Pietzsch T, Preibisch S, Rueden C, Saalfeld S, Schmid B, Tinevez JY (2012) Fiji: an open-source platform for biological-image analysis. Nat Methods 9(7):676–682. https://doi.org/10.1038/nmeth.2019

Schneider CA, Rasband WS, Eliceiri KW (2012) NIH image to ImageJ: 25 years of image analysis. Nat Methods 9(7):671–675. https://doi.org/10.1038/nmeth.2089

Schoonjans T, Brunetti A, Golosio B, del Rio MS, Solé VA, Ferrero C, Vincze L (2011) The xraylib library for X-ray–matter interactions. Recent developments. Spectrochim Acta b 66(11–12):776–784. https://doi.org/10.1016/j.sab.2011.09.011

Solé VA, Papillon E, Cotte M, Walter P, Susini J (2007) A multiplatform code for the analysis of energy-dispersive X-ray fluorescence spectra. Spectrochim Acta B 62:63–68. https://doi.org/10.1016/j.sab.2006.12.002

Soussou S, Mahieu S, Brunel B, Escarré J, Lebrun M, Banni M, Boussetta H, Cleyet-Marel JC (2013) Zinc accumulation patterns in four *Anthyllis vulneraria* subspecies supplemented with mineral nitrogen or grown in the presence of their symbiotic bacteria. Plant Soil 371:423–434. https://doi.org/10.1007/s11104-013-1698-9

Stein RJ, Höreth S, de Melo JRF, Syllwasschy L, Lee G, Garbin ML, Clemens S, Krämer U (2017) Relationships between soil and leaf mineral composition are element-specific, environment-dependent and geographically structured in the emerging model *Arabidopsis halleri*. New Phytol 213:1274–1286. https://doi.org/10.1111/nph.14219

Sujkowska-Rybkowska M, Muszyńska E, Labudda M (2020) Structural adaptation and physiological mechanisms in the leaves of *Anthyllis vulneraria* L. from metallicolous and non-metallicolous populations. Plants 9:662. https://doi.org/10.3390/plants9050662

Sujkowska-Rybkowska M, Lisek A, Sumorok B, Derkowska E, Szymańska M, Sas-Paszt L (2023) Arbuscular mycorrhizal fungi as an important factor enabling the adaptation of *Anthyllis vulneraria* L. to Zn-Pb-polluted tailings. Plants 12:2092. https://doi.org/10.3390/plants12112092

Tang YT, Sterckeman T, Echevarria G, Morel JL, Qiu RL (2019) Effects of the interactions between nickel and other trace metals on their accumulation in the hyperaccumulator *Noccaea caerulescens*. Environ Exp Bot 158:73–79. https://doi.org/10.1016/j.envexpbot.2018.11.015

Tang RH, Erskine PD, Nkrumah PN, Echevarria G, van der Ent A (2022a) Soil-plant relationships of metallophytes of the zinc-lead-copper Dugald River gossan, Queensland, Australia. Plant Soil 471:227–245. https://doi.org/10.1007/s11104-021-05209-z

Tang RH, Nkrumah PN, Erskine PD, van der Ent A (2022b) Polymetallic (zinc and cadmium) hyperaccumulation in the legumes *Crotalaria novae-hollandiae* and *Crotalaria*

cunninghamii. Plant Soil 479:589–606. https://doi.org/10.1007/s11104-022-05547-6

US Geological Survey (2026) Mineral commodity summaries 2026 (ver. 1.1, March 2026). U.S. Geological Survey. https://doi.org/10.3133/mcs2026

van der Ent A, Kopittke PM, Schat H, Chaney RL (2024) Hydroponics in physiological studies of trace element tolerance and accumulation in plants focussing on metallophytes and hyperaccumulator plants. Plant Soil 501:573–594. https://doi.org/10.1007/s11104-024-06537-6

Vasse J, De Billy F, Camut S, Truchet G (1990) Correlation between ultrastructural differentiation of bacteroids and nitrogen fixation in alfalfa nodules. J Bacteriol 172:4295–4306. https://doi.org/10.1128/jb.172.8.4295-4306.1990

White PJ (2016) Selenium accumulation by plants. Ann Bot 117:217–235. https://doi.org/10.1093/aob/mcv180

White PJ, Whiting SN, Baker AJM, Broadley MR (2002) Does zinc move apoplastically to the xylem in roots of *Thlaspi caerulescens*? New Phytol 153:201–207

Xiao T, Yang F, Li S, Zheng B, Ning Z (2012) Thallium pollution in China: a geo-environmental perspective. Sci Total Environ 421:51–58. https://doi.org/10.1016/j.scitotenv.2011.04.008

Xing JP, Jiang RF, Ueno D, Ma JF, Schat H, McGrath SP, Zhao FJ (2008) Variation in root-to-shoot translocation of cadmium and zinc among different accessions of the hyperaccumulators *Thlaspi caerulescens* and *Thlaspi praecox*. New Phytol 178:315–325. https://doi.org/10.1111/j.1469-8137.2008.02376.x

Yruela I (2013) Transition metals in plant photosynthesis. Metallomics 5:1090–1109. https://doi.org/10.1039/c3mt00086a

Zhang C, Charrois L, Jacquet J, Sirguey C, Chen Z, van der Ent A (2026) Monochromatic X-ray fluorescence spectroscopy for major and trace element analysis in plant science applications. Plant Soil 518:105–120. https://doi.org/10.1007/s11104-025-07984-5

Zhong Q, Qi J, Liu J, Wang J, Lin K, Ouyang QE, Zhang X, Wei X, Xiao T, El-Naggar A, Rinklebe J (2022) Thallium isotopic compositions as tracers in environmental studies: a review. Environ Int 162:107148. https://doi.org/10.1016/j.envint.2022.107148

Publisher's Note Springer Nature remains neutral with regard to jurisdictional claims in published maps and institutional affiliations.

Springer Nature or its licensor (e.g. a society or other partner) holds exclusive rights to this article under a publishing agreement with the author(s) or other rightsholder(s); author self-archiving of the accepted manuscript version of this article is solely governed by the terms of such publishing agreement and applicable law.